

Optical rogue wave statistics in laser filamentation

KASPARIAN, Jérôme, *et al.*

Abstract

We experimentally observed optical rogue wave statistics during high power femtosecond pulse filamentation in air. We characterized wavelength-dependent intensity fluctuations across 300 nm broadband filament spectra generated by pulses with several times the critical power for filamentation. We show how the statistics vary from a near-Gaussian distribution in the vicinity of the pump to a long tailed “L-shaped” distribution at the short wavelength and long wavelength edges. The results are interpreted in terms of pump noise transfer via self-phase modulation.

KASPARIAN, Jérôme, *et al.* Optical rogue wave statistics in laser filamentation. *Optics express*, 2009, vol. 17, no. 14, p. 12070-12075

DOI : 10.1364/OE.17.012070

Available at:

<http://archive-ouverte.unige.ch/unige:54907>

Disclaimer: layout of this document may differ from the published version.



Optical rogue wave statistics in laser filamentation

Jérôme Kasparian^{1*}, Pierre Béjot¹, Jean-Pierre Wolf¹ and John M. Dudley²

¹GAP GAP-Biophotonics, University of Geneva, 20, 1211 Geneva 4 Switzerland

²Institut FEMTO-ST, UMR 6174 CNRS-Université de Franche-Comté, Besançon, France

*Corresponding author: jerome.kasparian@unige.ch

Abstract: We experimentally observed optical rogue wave statistics during high power femtosecond pulse filamentation in air. We characterized wavelength-dependent intensity fluctuations across 300 nm broadband filament spectra generated by pulses with several times the critical power for filamentation. We show how the statistics vary from a near-Gaussian distribution in the vicinity of the pump to a long tailed “L-shaped” distribution at the short wavelength and long wavelength edges. The results are interpreted in terms of pump noise transfer via self-phase modulation.

©2009 Optical Society of America

OCIS codes: (190.4380) Nonlinear optics, four-wave mixing; (190.5530) Pulse propagation and solitons; (190.5940) Self-action effects; (190.7110) Ultrafast nonlinear optics

References and links

1. D. R. Solli, C. Ropers, P. Koonath, and B. Jalali, “Optical rogue waves” *Nature* **450**, 1054 (2007).
2. A. I. Dyachenko and V. E. Zakharov, “Modulation instability of Stokes wave implies a freak wave”, *JETP Lett.*, **81**, 255-259 (2005).
3. J. M. Dudley, G. Genty, and B. J. Eggleton, “Harnessing and control of optical rogue waves in supercontinuum generation,” *Opt. Express* **16**, 3644-3651 (2008).
4. D. R. Solli, C. Ropers, and B. Jalali, “Active control of optical rogue waves for stimulated supercontinuum generation,” *Phys. Rev. Lett.* **101**, 233902 (2008).
5. G. Genty, J. M. Dudley, B. J. Eggleton, “Modulation control and spectral shaping of optical fiber supercontinuum generation in the picosecond regime,” *Appl. Phys. B* **94**, 187-194 (2009)
6. C. Lafargue, J. Bolger, G. Genty, F. Dias, J. M. Dudley, B. J. Eggleton, “Direct detection of optical rogue waves energy statistics in supercontinuum generation,” *Electron. Lett.* **45**, 217-219 (2009)
7. N. Akhmediev, A. Ankiewicz, M. Taki, “Waves that appear from nowhere and disappear without a trace,” *Phys. Lett. A* **373**, 675-678 (2009)
8. N. Akhmediev, J. M. Soto-Crespo and A. Ankiewicz, “Extreme waves that appear from nowhere: on the nature of rogue waves”, *Phys. Lett. A*, doi:10.1016/j.physleta.2009.04.023 (2009)
9. D. Borlaug, S. Fathpour, B. Jalali, “Extreme value statistics and the Pareto distribution in silicon photonics,” arXiv:0809.2565v1 [physics.optics] (2008)
10. K. Hammani, C. Finot, J. M. Dudley and G. Millot, “Optical rogue-wave fluctuations in fiber Raman amplifiers,” *Opt. Express* **16**, 16467-16474 (2008)
11. S. L. Chin, S. A. Hosseini, W. Liu, Q. Luo, F. Théberge, N. Akozbek, A. Becker, V. P. Kandidov, O. G. Kosareva, and H. Schroeder, “The propagation of powerful femtosecond laser pulses in optical media: physics, applications, and new challenges,” *Can. J. Phys.* **83**, 863-905 (2005)
12. A. Couairon and A. Mysyrowicz. “Femtosecond filamentation in transparent media,” *Phys. Rep.* **44**, 47-189, (2007)
13. L. Bergé, S. Skupin, R. Nuter, J. Kasparian, and J.-P. Wolf. “Ultrashort filaments of light in weakly ionized, optically transparent media,” *Rep. Prog. Phys.* **70**, 1633-1713, (2007)
14. J. Kasparian and J.-P. Wolf. Physics and applications of atmospheric nonlinear optics and filamentation. *Opt. Express* **16**, 466-493, (2008)
15. P. Béjot, J. Kasparian, E. Salmon, R. Ackermann, J.-P. Wolf, “Spectral correlation and noise reduction in laser filaments,” *Appl. Phys. B* **87**, 1-4 (2007)
16. S. Coles, *An Introduction to Statistical Modeling of Extreme Values*, Springer-Verlag, London, (2001).
17. V. Pareto, “*Manuale di economia politica con una introduzione alla scienza sociale*”, Societa Editrice Libreria, Milano (1906)

18. S. Bendersky, N. S. Komeika, and N. Blaunstein, "Atmospheric Optical Turbulence Over Land in Middle East Coastal Environments: Prediction Modeling and Measurements," *Appl. Opt.* **43**, 4070-4079 (2004)
19. R. Salamé, N. Lascoux, E. Salmon, J. Kasparian, and J.P. Wolf, "Propagation of laser filaments through an extended turbulent region," *Appl. Phys. Lett.* **91**, 171106-171106 (2007)

1. Introduction

There has recently been much interest in the study of extreme value or "rogue" events in nonlinear optics. Such events are associated with characteristic heavy tailed "L-shaped" probability distributions where – in stark contrast to Gaussian statistics – events much larger than the mean occur with significant probability. Initial interest in this area began in late 2007 with experiments reporting extreme value events in fiber supercontinuum generation associated with the generation of high power soliton pulses [1]. These experiments attracted widespread attention because they were carried in a regime where the spectral broadening was seeded by modulation instability, allowing important links to be made with mechanisms potentially underlying the formation of oceanic rogue waves [2].

Within the optics community, these results rapidly initiated studies into techniques for supercontinuum stabilization in the presence of noise [3-6]. Complementary work has explored non-soliton mechanisms for rogue wave formation in optical fibers, associated with the propagation dynamics and collisions of nonlinear breathers [7-8]. Aside from systems where direct analogy with oceanic waves can be drawn, other research has found that long-tailed distributions with similar extreme value or rogue wave-like statistics can appear in systems such as fiber Raman amplification and silicon photonics [9-10].

In this paper, we report a further example of nonlinear propagation exhibiting long tailed statistics characteristic of extreme value processes, thus confirming that such behavior may be very widespread in optical systems. Specifically, we study intensity fluctuations across the spectrum of a self-guided optical filament generated with pulses close to the critical power for filamentation in air [11-14]. In contrast to the experiments in fiber supercontinuum generation [1], we do not characterize the ultrafast temporal structure of the filament fluctuations, but rather characterize the wavelength dependence of the shot-to-shot intensity fluctuations across the generated filament spectrum. Our results show how the statistics vary from a near-Gaussian distribution near the center of the spectrum to long-tailed at the short wavelength and long wavelength edges. A simple numerical model is used to interpret these results in terms of pump noise transfer via self-phase modulation.

2. Experimental set-up

The experimental setup has been previously described in detail in [15], but is shown in Fig. 1 for completeness. A CPA (Chirped Pulse Amplification) Ti:Sapphire laser system delivers 200 fs pulses with pulse energy in the 1-6 mJ range (5-30 GW peak power). The centre wavelength is 815 nm and the beam diameter (at $1/e^2$ level) is around 10 mm.

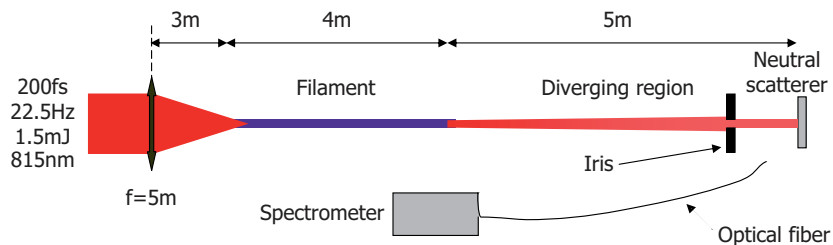


Fig. 1. Experimental setup

The beam was focused by a spherical mirror with 5 m focal length, yielding a non-linear focus (filament onset) ~ 3 m downstream of the spherical mirror. Self-guided filaments typically 4 m long were generated. A pinhole selected the supercontinuum emitted by the filament, rejecting the surrounding “photon bath” and conical emission. We checked that the filament pointing stability was sufficient to prevent truncation of the supercontinuum by the iris. The supercontinuum was then scattered onto a spectrally neutral target, and the scattered light was collected using a fiber. Its spectrum was recorded at 3 nm resolution using a fiber spectrometer. For a range of different power levels as described below, an ensemble of 5000 spectra was sampled. The sampling rate of ~ 5 Hz was lower than the source repetition rate because of detection latency time of 200 ms, but each measured spectrum corresponded to one distinct input pulse with no averaging effect. We can record individual spectra in this way because of the low repetition rate of the source, and this represents a complementary technique to the ultrafast detection techniques that have been used to characterize soliton rogue wave events with high repetition rate fiber sources.

3. Experimental results

Figure 2(a) shows a series of experimentally measured spectra obtained at the filament output for a pulse peak power of $P_0 = 15 \text{ GW} = 5 P_{cr}$, where $P_{cr} = 3 \text{ GW}$ is the critical self-focusing power for air. We plot only 500 realizations from the full ensemble for clarity. As expected under these pumping conditions, the mean spectrum (bold line) exhibits significant spectral broadening. However, it is also clear from the distribution of individual spectra (gray curves) that there are considerable shot-to-shot fluctuations at wavelengths away from the 815 nm pump. Towards the spectral edges, this leads to considerable jitter in the overall filament spectral width. The qualitative differences in the fluctuations near the pump and at the edges are illustrated in Fig. 2(b) and (c) which shows the equivalent time series of the filtered intensity at wavelengths of 815 nm and 630 nm respectively.

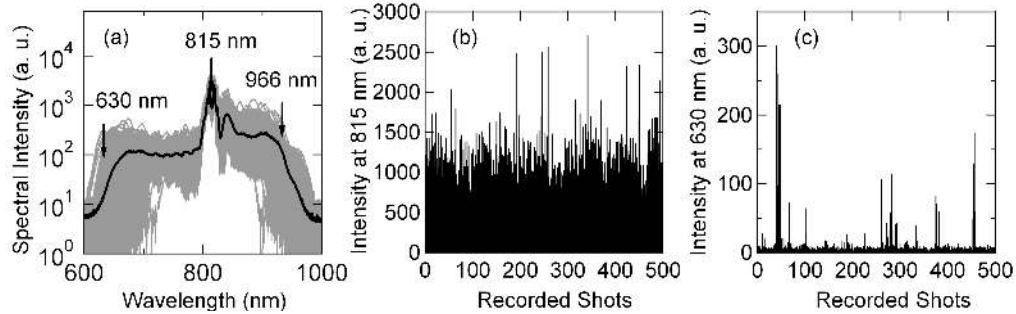


Fig. 2 (a) Typical series of 500 individual spectra (gray traces), together with the calculated mean over the same 500-shot ensemble (bold line). These results were measured at the output of a filament generated by a 15 GW (*i.e.* $5 P_{cr}$) pump. (b) and (c) show time series of the intensity at (b) 815 nm in the spectrum center, and (c) 630 nm on the spectrum edge.

These noise properties were examined in more quantitative detail by calculating the histograms of the intensity fluctuations at the three different wavelengths marked on Fig. 2(a). These results are shown in Fig. 3, and clearly show significant differences between the spectral centre and wings. Specifically, At 815 nm near the pump, we see a near-Gaussian distributed fluctuations, whereas on the edges of the supercontinuum at 630 nm and 966 nm, L-shaped long-tailed histograms characteristic of extreme-value behavior are observed. Although a detailed analysis of the exact nature of these statistical properties is outside the scope of this paper, we have checked that these histograms are fitted (at 5% confidence levels) by distributions such as Weibull or Pareto that are commonly associated with long tailed behavior [16]. Note that the null hypothesis of a Gaussian distribution fit to these histograms was rejected even at the 20% confidence level.

To gain improved insight into the mechanisms leading to these extreme non-Gaussian distributions, we have also characterized the distribution of the intensity fluctuations at all wavelengths across the spectrum, not only at specific wavelengths shown in Fig. 3. Significantly, such a full analysis of the wavelength dependence of the fluctuations is possible with our particular setup that allows a large number of shot-to-shot spectral measurements, but has not been possible in the earlier work studying fiber supercontinuum generation at higher repetition rates.

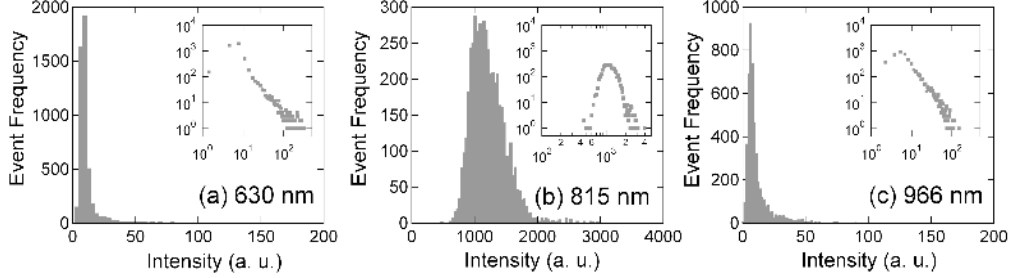


Fig. 3 Histograms at (a) 630 nm (b) 815 nm and (c) 966 nm. Insets show the same data on a log-log representation to highlight the differences in the distributions – while the distribution in (b) is bell-shaped, the distributions on the edges exhibit L-shaped characteristics.

To perform such a wavelength-dependent analysis, we introduce a long-tailed “Pareto-like” metric that can be readily computed from the experimental data. Specifically, we recall that long tailed distributions are often characterized by relationships such as the Pareto Principle which states that a large fraction (typically 80%) of the events or effects under study are associated with a small (typically 20%) of the causative factors [17]. Of course, the two quantities compared in the Pareto ratio are dimensionally different, and the ratio of 80/20 is arbitrary, but it is nonetheless a very useful concept to characterize the tendency of a particular distribution to exhibit extreme value or long-tailed characteristics. In quantitative terms, we consider the ensemble of spectra obtained $[I_n(\lambda)]$ with $n = 1 \dots N$ ($N = 5000$ in our case). At the considered wavelength λ_0 we sort the spectra by decreasing values so that $I_0(\lambda_0) > I_1(\lambda_0) > I_2(\lambda_0) > \dots > I_N(\lambda_0)$ and then compute the “Pareto Metric” at λ_0 , defined by:

$$M(\lambda_0) = \frac{\sum_{i=1}^{kN} I_i(\lambda_0)}{\sum_{i=1}^N I_i(\lambda_0)} \quad (1)$$

where the first sum corresponds the kN most intense measurements at the considered wavelength, with $k = 0.2$ is taken for consistency with the Pareto Principle. In physical terms, this yields the contribution of the kN most intense measurements to the average signal. The lowest possible value of the metric is $M = k$ in the case of a uniform distribution, $M \approx 0.44$ for a Gaussian distribution, whilst values of $M > 0.5$ indicate substantial deviation from Gaussian statistics and the development of an asymmetric long-tailed probability density function.

Figure 4 shows our results characterising the wavelength dependence of the intensity fluctuations in this manner. Here we plot both the evolution of the mean filament spectrum and the corresponding metric $M(\lambda)$ for a range of input peak powers. There are two main points to draw from these results. Firstly, the metric M is higher towards the spectral edges than near the centre, confirming the association between nonlinear spectral broadening and deviation from Gaussian statistics. Secondly (and quantitatively) the metric increases to $M > 0.5$ where we see characteristic long-tailed histogram behavior for power levels exceeding $3.7 P_{cr}$ and, moreover, the maximum value of M anywhere across the spectrum also increases with power, taking values of 0.52, 0.62 and 0.73 for power levels of $3.7 P_{cr}$, $5 P_{cr}$ and $5.5 P_{cr}$ respectively. These results extend those shown in Fig. 3 in clearly showing the difference in intensity distributions as a continuous function of wavelength across the spectrum.

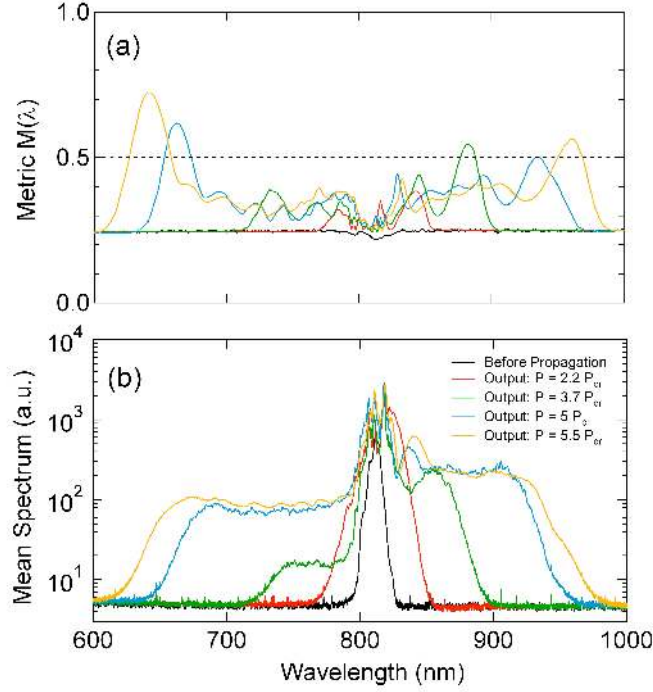


Fig. 4 Filament spectra for peak powers as shown. (a) plots the wavelength-dependence of the metric $M(\lambda)$ and (b) shows the corresponding spectra. Values of $M > 0.5$ (dotted line) indicate the development of a long tail on the probability distribution.

4. Discussion and interpretation

The increase in the Pareto metric towards the spectrum edges of the spectrum and with higher input power indicates strong correlation between nonlinear spectral broadening in the filament and the appearance of long-tailed statistics. This is a further example of an optical system in which nonlinearity generates extreme-value behaviour, complementing other recent studies in other systems [9, 10]. Significantly, although a complete description of filament supercontinuum generation is complex, a satisfactory qualitative interpretation of our results above can be obtained assuming that spectral broadening is dominated by self-phase modulation (SPM). We have numerically calculated the output spectrum after SPM by calculating the intensity-dependent non-linear phase imposed to each temporal slice of the pulse and computing the Fourier transform of the output electric field. The considered intensity of $5 \times 10^{13} \text{ W/cm}^2$ [11-14], propagation distance of 5 cm (typical of the distance over which the initial SPM-dominated broadening occurs), pulse duration of 100 fs, and nonlinear refractive index of air, $n_2 = 2.84 \times 10^{-19} \text{ cm}^2/\text{W}$ were typical of filamentation. We performed 1000 realisations with Gaussian-distributed intensity noise (at $\pm 2\%$ standard deviation) and wavelength jitter ($\pm 3 \text{ nm}$ standard deviation), yielding an ensemble of 1000 spectra.

The mean spectrum and the corresponding Pareto-metric from Eq. (1) are shown in Fig. 5. Although we would not expect a simplified SPM-based model to be quantitatively accurate, the results nonetheless show that noise-driven SPM broadening provides a good qualitative description of the spectral characteristics measured in our experiments. In particular, the increase in the M-metric towards the spectral edges and the associated deviation from Gaussian to long-tailed L-shaped statistics are well-reproduced in our simulations. Reproducing the simulation with different intensity and wavelength jitters, we found that both parameters combine additively to generate a L-shaped statistics. However, for intensity and wavelength noises typical of CPA laser chains, the individual contribution of the wavelength jitter contributes more efficiently to the generation of an L-shaped statistics.

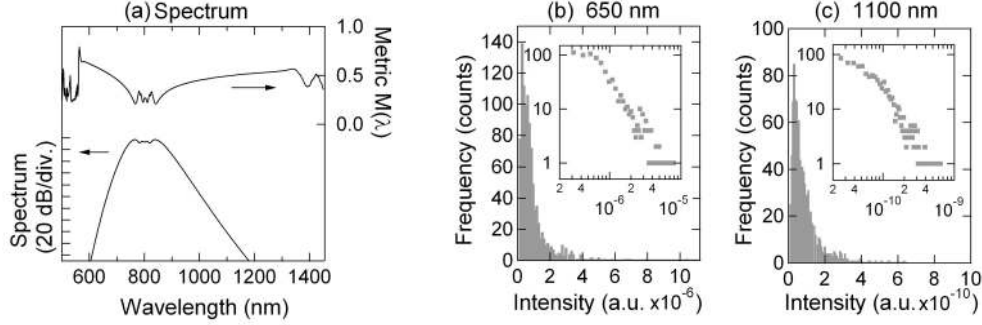


Fig. 5 (a) Mean spectrum (log scale, left axis) and Pareto metric $M(\lambda)$ (right axis) for 1000 realizations of noise-induced SPM. Peak spectral intensity is 57 dB. (b) and (c) Histograms of spectral intensities at 650 nm and 1100 nm respectively. Insets use a log-log representation.

It is important to stress, however, that although these results are certainly suggestive of the dominant role of SPM in transforming Gaussian pump noise into L-shaped statistics, the filamentation process itself involves a number of other processes whose role necessitates further study. In particular, we note that our experimental filtering of conical emission from the measurements may potentially exclude noise contributions due to plasma effects.

We also investigated experimentally the effect of additional noise sources in the system, specifically inserting a strong turbulence area ($C_n^2 \gg 10^9 \text{ m}^{-2/3}$, $\sim 10^4$ times the highest atmospheric values [18]) over 1 m along the propagation region. We previously reported that filaments propagate almost unaffected in such conditions [19]. We observed that the turbulence leads to two competing effects depending on input power. In the low-power regime ($2.9 P_{cr}$), turbulence affects only marginally the spectral dependence of the Pareto-metric in Fig. 4(b). At higher power ($7.5 P_{cr}$), strong turbulence destroys typically 90 % of the filaments. The intensity distribution in a given wavelength range is therefore governed by whether or not a filament is formed. In this distribution, high intensities at any wavelength correspond to the occurrence of a filament, whose formation can then be considered as an extreme (“rogue”) event. The intensity distribution is therefore L-shaped not only on the edges of the spectrum, but also over the *whole* spectrum, including around the central wavelength where the Pareto-metric increases beyond 0.5.

5. Conclusions

The major result presented here has been the experimental observation of optical rogue wave statistics in the self-guided filamentation of high-power femtosecond pulses propagating in both still and highly turbulent air. Our experiments are in contrast to the ultrafast measurement techniques used to directly characterize rogue wave soliton pulses on the long wavelength edge of fiber supercontinuum spectra. Rather, we record an ensemble of broadband filament spectra and characterize the wavelength-dependence of the intensity fluctuations across the 300 nm broad white-light continuum. By introducing a convenient Pareto-like metric, we have shown how the statistics vary from a near-Gaussian distribution in the vicinity of the pump to a long tailed “L-shaped” distribution at the short wavelength and long wavelength edges. Based on a simple numerical model, we have interpreted our results in terms of pump noise transfer via self-phase modulation.

Acknowledgements

This work was supported by the *Institut Universitaire de France*, the *Agence Nationale de la Recherche* Project MANUREVA (ANR-08-SYSC-019), the *Fonds National Suisse de la Recherche Scientifique* (FNS, grant #200021-116198/1), and the *Swiss Secrétariat d'État à l'Éducation et à la Recherche* in the framework of the COST P18 project “The Physics of Lightning Flash and its Effects”.